2019 International Symposium on Lightning Protection (XV SIPDA), São Paulo, Brazil, 30th September – 4th October 2019.

Simulation of Lightning Transients in Large Wind Farms

Rafael Alipio, Miguel Guimarães, Lucas Passos, Daiane Conceição
DEE/CEFET-MG
Federal Center of Technological Education, Belo Horizonte, MG, Brazil
rafael.alipio@cefetmg.br

M. T. Correia de Barros
Instituto Superior Técnico (IST)
University of Lisbon (UL)
Lisbon, Portugal
teresa.correiadebarros@tecnico.ulisboa.pt

Marco Aurélio de O. Schroeder
Department of Electrical Engineering (DEPEL)
Federal University of São João del-Rei (UFSJ)
São João del-Rei, Brazil
schroeder@ufsj.edu.br

***Abstract*—This paper proposes an accurate and efficient approach for simulating transients in large wind farms, considering a hybrid approach based on electromagnetic field theory and EMTP-type programs. A case-study comprising five wind turbines, with the individual grounding systems of the wind turbines interconnected through bare cables, is assessed. The Ground Potential Rise (GPR) and the transferred voltages to the adjacent grounding systems are calculated considering the injection of currents representative of first and subsequent strokes. The need of accurately modelling the individual towers grounding systems and interconnecting electrodes is evaluated. It is shown that the use of simplified approaches leads to overestimating the transient voltages developed in the wind farm in response to lightning currents.**

Keywords—Wind farm; Interconnected Grounding Systems; Lightning response; Ground Potential Rise; Transient simulation.

I. INTRODUCTION

Due to their height and typical installation sites, wind turbines (WT) are preferential points of lightning incidence. According to statistics presented in [1], 40% to 50% of lightning faults at wind turbines have involved damage to control systems and sensitive electronic equipment. The wind turbine grounding, bonding, and lightning protection systems play an important role and provide protection of electrical equipment and personnel [1], [2]. Furthermore, these systems provide reduction of electrical noise and proper operation of electrical and electronic communications and control equipment [2].

Even following good practices in designing the wind turbine lightning protection system (LPS), additional studies may be necessary, namely transient studies associated with lightning occurrences in the wind farm [3], [4]. It is important to determine the Grounding Potential Rise (GPR) developed by the grounding system of a wind turbine struck by lightning, which can be transferred to the power grid through the step-up transformer installed in each WT [5], [6]. Also, it is important to accurately determine the potential distribution along the grounding system of the wind farm, which cannot be assumed an equipotential under transients [7]. Furthermore, it is important to determine the transient distribution of current along the tower body. This is relevant from the point of view of the electromagnetic compatibility (EMC), in order to predict the electromagnetic fields inside the wind turbine and their induction effects that can cause malfunction of sensible electronic equipment.

The accurate simulation of electromagnetic transients in a wind farm presents certain complexities. A wind farm may be composed of several wind turbines operating together and being separated by a distance in the order of the rotor diameter. Normally, the grounding systems of the individual wind turbines are interconnected through long buried horizontal electrodes, as recommended in the IEC standard TR61400-24 [1]. In order to accurately simulate the lightning transients in a wind farm, such aspects should be taken into account. However, the large dimensions involved in a wind farm renders the use of a full wave model too cumbersome or unfeasible, due to computational constraints, mainly considering differential numerical methods such as FDTD [8].

This paper aims at presenting a contribution to the simulation of lightning transients in wind farms. In this context, the objective of the paper is twofold. First, to propose an accurate and efficient approach for simulating transients in a wind farm, considering a hybrid approach based on electromagnetic field theory and EMTP-type programs. Second, to assess the accuracy of simplified models of interconnected grounding systems commonly used for simulating electromagnetic transients in wind farms.

The paper is organized as follows. Modeling details and the simulated system are described in Section II. Section III presents the obtained results. Conclusions are finally presented in Section IV.

This work has been supported by the Brazilian agencies FAPEMIG (TEC-APQ-02017-16) and CNPq (312763/2018-2).

II. CASE-STUDY AND MODELING GUIDELINES

A system composed of five wind turbines is considered, as depicted in Fig. 1. Each wind turbine (WT) is sustained by a 60-m height metallic tower with a 3-m base diameter, which is connected to the grounding system with a typical octagonal configuration whose dimensions are indicated in Fig. 2. The grounding systems of the individual wind turbines are interconnected through a 200-m long bare cable. A soil resistivity value of 500 Ωm is assumed.

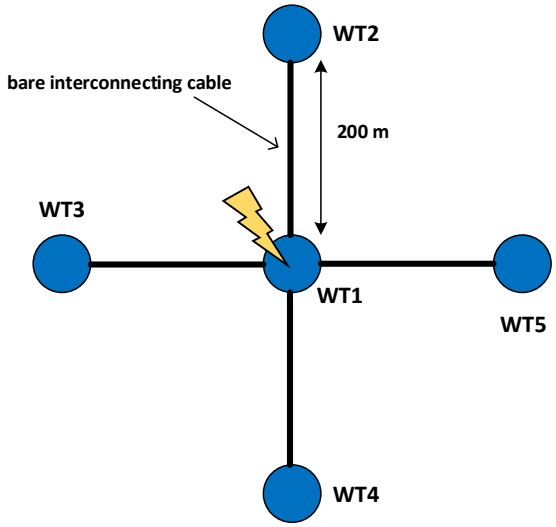

Fig. 1. Simulated wind farm.

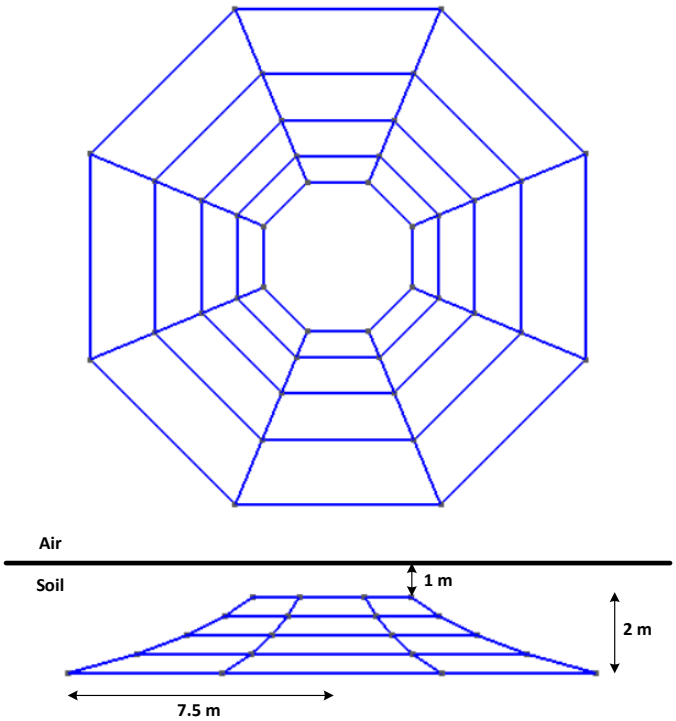

Fig. 2. Wind turbine grounding system.

The lightning current is injected at the top of the tower of the central wind turbine (WT1) and the following quantities are calculated: i) the GPR developed at the struck tower (WT1); and ii) the transferred voltage to the adjacent tower (WT2).

All simulations are developed in the Alternative Transients Program (ATP) [9]. Modeling of soil parameters, wind turbine tower, grounding system, interconnecting electrode and lightning current is described below.

A. *Tower Modeling*

Normally, a typical WT tower comprises either three or four main tower sections that are joined together in the field with bolted flanges. In this paper, the tower height of the considered WTs is lt=60 m and is divided into four main sections, as depicted in Fig. 3. The dimensions of each section are presented in Table I.

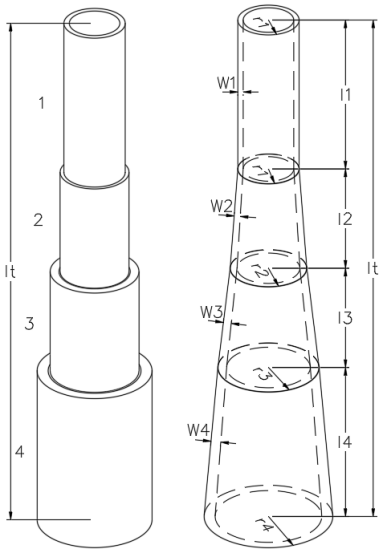

Fig. 3. Wind turbine tower.

TABLE I. DIMENSIONS OF EACH SECTION OT THE WIND TURBINE TOWER

Section		Diameter (m)	Thickness (cm)
Number	*Length (m)*		
4	0-15	3.00	5.00
3	15-30	2.50	4.40
2	30-45	2.20	3.50
1	45-60	1.80	2.80

Each section of the tower is modelled as a lossless single-phase transmission line, for which the surge impedance is calculated using the revised Jordan's formula, which was extended in [10] to take into account vertical multiconductor systems. Each section is represented by n parallel vertical conductors distributed along its perimeter. Assuming that the current is equally distributed among these conductors, it is possible to represented the whole multiconductor system associated with a section as a single transmission line with equivalent surge impedance Z_{eq} given by [10]

$$Z_{eq} = \frac{V}{I} = \frac{Z + Z_{12} + Z_{13} + ... + Z_{1n}}{n} \quad (1)$$

where

$$Z = 60\left[\ln\frac{4h}{r} - 1\right] \quad (2)$$

$$Z_{ij} = 60\ln\frac{2h + \sqrt{4h^2 + {d_{ij}}^2}}{{d_{ij}}^2} + 30\frac{d_{ij}}{h} - 60\sqrt{1 + \frac{{d_{ij}}^2}{4h^2}} \quad (3)$$

In (2) and (3), h is the height of the conductor, r is the conductor radius, and d_{ij} corresponds to the distance between the centers of conductors i and j. For the tower shown in Fig. 3, each section was represented by n=50 parallel conductors equally spaced and distributed along the perimeter of the corresponding tower section, and the diameter of each one was assumed equal to the thickness of the corresponding section (W1 to W4 in Fig. 3). The following values were obtained for the surge impedance of each section of the tower:

Z_4=170 Ω, Z_2=219 Ω, Z_3=253 Ω, and Z_1=276 Ω.

B. Soil Modeling

According to experimental data obtained in both laboratory and field measurements, the soil conductivity σ_g and permittivity ε_g present a strong variation along the typical frequency range of lightning currents (0 Hz to few MHz) [11], [12]. The soil permeability, in general, can be assumed constant and equal to the vacuum permeability, μ_0 [11].

For modeling the frequency dependence of soil electrical parameters, the causal model proposed by Alipio and Visacro is used [12]. The model equations read

$$\sigma_g = \sigma_0 + \sigma_0 \times h(\sigma_0)\left(\frac{f}{1\ \text{MHz}}\right)^{\zeta} \quad (4)$$

$$\varepsilon_g = \varepsilon'_{\infty} + \frac{\tan(\pi\zeta/2)\times 10^{-3}}{2\pi(1\text{MHz})^{\zeta}}\sigma_0 \times h(\sigma_0) f^{\zeta-1} \quad (5)$$

In (4) and (5), σ_g is the soil conductivity in mS/m, $\sigma_0=1/\rho_0$ is the DC conductivity in mS/m, ε_g is the soil permittivity, ε'_{∞} is the soil permittivity at higher frequencies and f is the frequency in Hz. According to [12], the following parameters are recommended in (4) and (5) to obtain mean results for the frequency variation of σ_g and ε_g:

ζ=0.54, $\varepsilon'_{\infty}=12\varepsilon_0$ and $h(\sigma_0)=1.26\times\sigma_0^{-0.73}$

where ε_0 is the vacuum permittivity.

C. Grounding System Modeling

Lightning currents present a large frequency content, which can range from DC to few MHz. In this frequency range, grounding system shows a strong frequency-dependent behavior. In this paper, three different models are considered.

Accurate modelling – The frequency response of the grounding system of each individual wind turbine is expressed in terms of its harmonic impedance Z(s=jω), given by the ratio of the phasors of the GPR and injected current. The harmonic impedance is calculated in the frequency range of 1 Hz to 10 MHz using the accurate Hybrid Electromagnetic Model (HEM) [13], the soil parameters being assumed frequency-dependent as described in *B*.

The calculated harmonic grounding impedance Z(s=jω) is approximated by a pole–residue model using the Vector Fitting (VF) method [14]. Finally, a single-port linear electrical network that is suitable to time-domain simulations is derived from the obtained pole-residue model using the technique proposed in [15]. This electrical network is implemented in ATP, which can be used for an efficient time-domain simulation of large interconnected grounding considering the presence of other system components.

Simplified modelling – Two simplified grounding models are considered, the grounding system being represented by either the low-frequency resistance (R_{LF}) or the impulse impedance (Z_P), which is frequently used to characterize the surge behavior of grounding systems. The low-frequency resistance is calculated by the ratio of the GPR and injected current along the wave tail. The impulse impedance is calculated by the ratio of the GPR and injected current peaks.

D. Interconnecting Electrode Modeling

The distributed parameter nature of the interconnecting electrode must be considered, and two different models are used in this paper.

Accurate modelling – The interconnecting bare cable is modeled as a two-port electrical network representing the frequency response seen from its sending and receiving ends, which is obtained from field theory results obtained for the nodal admittance using HEM, in a frequency range from 1 Hz to 10 MHz. The soil parameters are assumed frequency-dependent according to the Alipio-Visacro causal model. From the frequency response, a pole-residue model is fitted using VF and a two-port electrical network representing the bare cable is obtained. This two-port network can be promptly included in ATP for time-domain simulations. Further details regarding the multiport electrical network synthesis can be found in [16].

Simplified modelling –The electrode is assumed to be a buried transmission line and is represented via the well-known nodal admittance matrix. For a line length ℓ, the characteristic admittance Y_c and the propagation function A, which are calculated using the line-impedance per unit of length Z and the line-admittance per unit length Y, are defined as

$$Y_c = Z^{-1}\sqrt{ZY} \quad (6)$$

$$A = \exp\left(-\ell\sqrt{ZY}\right) \quad (7)$$

The per-unit-length impedance, Z, and admittance, Y, are

$$Z = j\omega L \quad (8)$$

$$Y = G + j\omega C \quad (9)$$

where L, G and C are the per-unit-length inductance, conductance and capacitance, respectively (the longitudinal resistance per unit length R is disregarded, since its effect is negligible in the analysis of buried bare cables). Considering the classical expressions proposed by Sunde, the per-unit-length

conductance of a horizontal bare cable buried in soil can be computed by [17]

$$G = \sigma_g \pi \left[\log \frac{2\ell}{\sqrt{2da}} - 1 \right]^{-1} \quad (10)$$

where ℓ (in m) is the cable length, a (in m) is the cable radius, and d (in m) is the depth below ground. The cable per-unit-length capacitance is computed by considering the duality relationship between C and G, $C/G = \varepsilon_g / \sigma_g$ .The per-unit-length inductance is computed by

$$L = \frac{\mu}{2\pi} \left[\log \frac{2\ell}{a} - 1 \right] \quad (11)$$

where μ is the soil permeability (in H/m).

Finally, the nodal admittance matrix is given by

$$Y_n = \begin{bmatrix} Y_c \left(U + A^2\right)\left(U - A^2\right)^{-1} & -2Y_c A\left(U - A^2\right)^{-1} \\ -2Y_c A\left(U - A^2\right)^{-1} & Y_c \left(U + A^2\right)\left(U - A^2\right)^{-1} \end{bmatrix} \quad (12)$$

where U is the identity matrix.

In a similar way to that described when using the HEM model, the nodal admittance matrix is calculated in a frequency range from 1 Hz to 10 MHz, assuming frequency-dependent soil parameters. From the frequency response, a pole-residue model is fitted using VF and a two-port electrical network representing the interconnecting bare cable is obtained.

E. Lightning Current

Typical downward lightning currents are considered. According to measurements performed in instrumented towers, first stroke currents of downward negative lightning are characterized by a pronounced concavity at the front and by the occurrence of multiple peaks [18]. Generally, the second peak presents the highest current amplitude, whereas the maximum steepness occurs near the first peak. The waveform of most subsequent negative downward strokes presents a single peak and a relatively smooth shape. Accordingly, the current waveforms illustrated in Fig. 4 [18], which closely reproduces the median parameters of first and subsequent negative downward strokes measured at Mount San Salvatore [19], are used in the simulations.

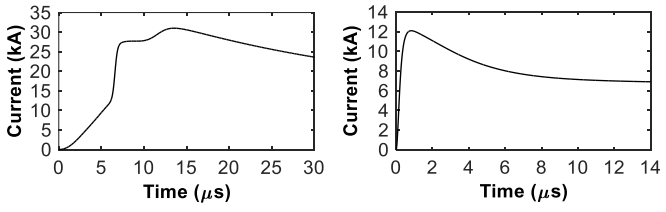

(a) (b)

Fig. 4. Representative current waveforms of first (a) and subsequent (b) negative downward strokes measured at Mount San Salvatore.

III. RESULTS

Results were computed considering three different modelling options for the wind turbine grounding system and interconnecting electrode:

- Field Theory –the accurate models are used for both the wind turbine grounding systems and interconnecting electrodes;
- TL Theory + Z_P – the individual turbine grounding systems are represented by a lumped resistance of value equal to the impulse impedance Z_P=9.4 Ω and the interconnecting electrodes by a frequency-dependent model obtained from a transmission line theory approach
- TL Theory + R_{LF} – same as previous for the interconnecting electrodes, and the grounding system is represented by a lumped resistance of value equal to the low-frequency resistance R_{LF}=13.5 Ω.

Note that Z_P is lower than R_{LF} because of the frequency dependence of soil parameters [20].

In all cases, the wind turbine tower is represented according to the model described in Section II-A and the impulse currents illustrated in Fig. 4 are injected at the tower top of the central wind turbine (WT1 in Fig. 1).

A. Ground Potential Rise (GPR)

Fig. 5 and Fig. 6 show the GPR at the struck tower, considering the three different modelling options, in response to first and subsequent strokes, respectively.

According to the results, the GPR waveform presents an initial oscillatory behavior, which is attributed to the multiple reflections that take place at the top of the struck tower. Such oscillatory behavior is more expressive in case of the GPR in response to subsequent strokes. After this oscillatory period, the GPR shows a smooth behavior. Interestingly, although the amplitude of the first stroke current is around 2.6 times greater than that of the subsequent stroke, the peak value of the GPR in response to first stroke is around 1.6 times greater than that of the GPR in response to subsequent stroke, assuming field theory as reference. Due to the high frequency content of the lightning currents, the propagation effects, with emphasis on the attenuation, are relevant. Indeed, as a result of attenuation, only a small part of the grounding system around the injection point is seen by the lightning current, during the first microseconds of the transient [21]. Since first stroke currents are slower than subsequent stroke currents, they have a lower frequency content; then, the attenuation effects are less significant in the case of first strokes. Since waves are subjected to less attenuation effects, the area seen by the lightning current covers a larger perimeter, and the impulse efficiency of the grounding system is better for first strokes in comparison with subsequent strokes. This justifies why the ratio between the GPR peaks in response to first and subsequent strokes does not follow the same ratio between the associated currents.

It is to be noted that the GPR, which shows high values during the first microseconds of the transient, tends to very low values along the wavetail. This occurs because, along the wavetail, which is associated with low frequencies, the whole interconnected grounding system of the wind farm is seen by the

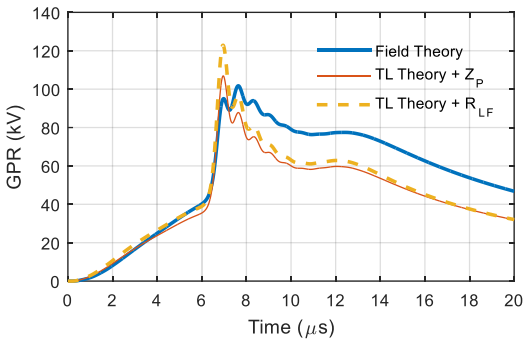

(a)

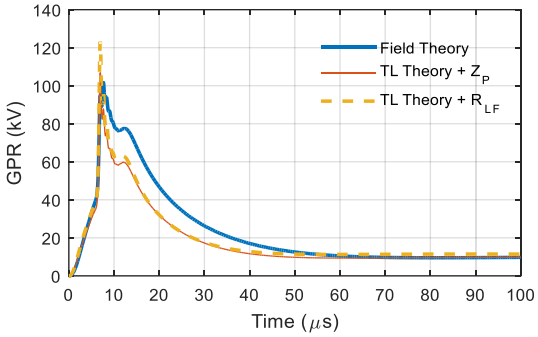

(b)

Fig. 5. GPR at the grounding system of the struck wind turbine, in response to first stroke current. (a) GPR during the first microseconds, and (b) Complete GPR waveform.

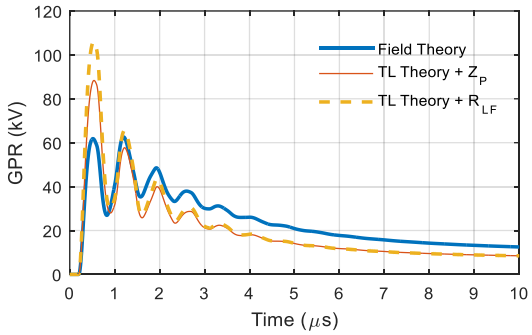

(a)

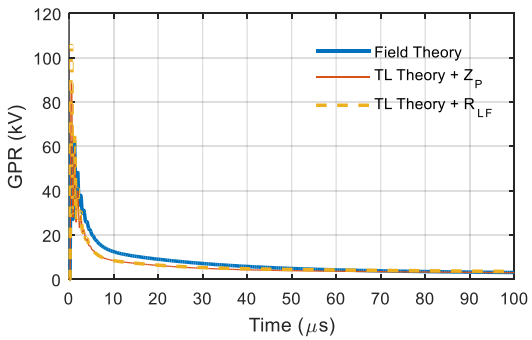

(b)

Fig. 6. Same as Fig. 5, but considering the injection of the subsequent stroke current.

lightning current. The low-frequency grounding resistance of the whole wind farm grounding system is quite low, justifying the lower values of GPR along the wavetail.

As regards the comparison of results obtained with the different modelling options, Fig. 5 and Fig. 6 show that the simplified representation of the grounding system by a lumped resistance, along with the use of the transmission line theory for modelling the interconnecting electrode, leads to results in disagreement with those obtained by using field theory based modeling. The main differences are observed during the first microseconds of the transient, when the GPR shows faster variations. Discrepancies are observed both in amplitude and waveform, especially in the case of the GPR developed in response to the subsequent stroke current. This shows the importance of rigorously modeling the frequency response of the grounding system and interconnecting electrodes, in order to accurately estimate the ground potential rise.

B. Transferred Voltages

Fig. 7 and Fig. 8 show the voltage that is transferred to the grounding system of the wind turbine WT2 in Fig. 1, considering the three different modelling options, for first and subsequent stroke currents, respectively.

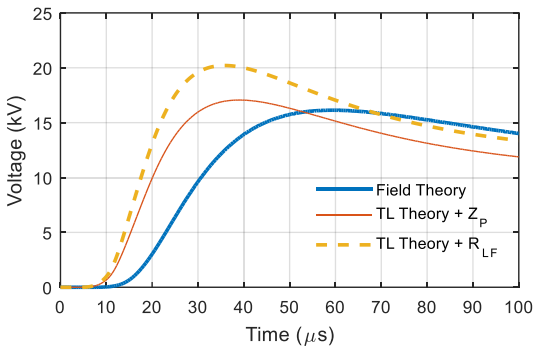

Fig. 7. Transferred voltage to the grounding system of the wind turbine WT2, considering the injection of first stroke current.

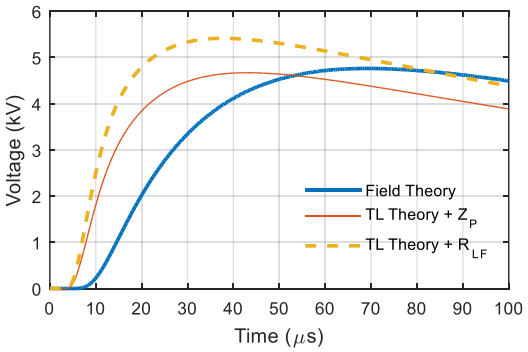

Fig. 8. Transferred voltage to the grounding system of the wind turbine WT2, considering the injection of subsequent stroke current.

Results show that the transferred voltage is attenuated and distorted, exhibiting a slower rise as compared to the GPR. The attenuation of the voltage waves is more significant in the case of subsequent strokes, since such currents have higher frequency

content. It is also seen that the transferred voltages calculated using the transmission line theory to model the interconnecting electrodes are in disagreement with those voltages predicted from field theory based modelling. Differences are observed both in amplitude and waveform, and also in terms of the wave travel time.

IV. Summary and Conclusions

An accurate and efficient approach was developed for simulating transients in large wind farms, considering a hybrid approach based on electromagnetic field theory and EMTP-type programs. In order to evaluate the need of accurately modelling the individual towers grounding systems and interconnecting electrodes, simplified models of these components are also considered: a lumped resistance for the first, and transmission line theory-based approach for the latest. A case-study comprising five interconnected wind turbines was considered, and it was shown that the use of simplified models leads to results in disagreement with those predicted using an accurate field theory approach. In all analyzed cases, the use of simplified models overestimates the calculated transient voltages, especially if the grounding system is represented by a lumped resistance with value equal to its low-frequency grounding resistance.

References

[1] "Wind turbine generator systems—Part 24: Lightning protection," IEC Tech Rep. 61400-24, 2010.

[2] V. T. Kontargyri, I. F. Gonos, and I. A. Stathopulos, "Study on Wind Farm Grounding System,"IEEE Trans. Industry Applications, vol. 51, no. 6, pp. 4969–4977, Nov./Dec. 2015.

[3] K. Yamamoto, S. Yanagawa, K. Yamabuki, S. Sekioka, and S. Yokoyama, "Analytical surveys of transient and frequency-dependent grounding characteristics of a wind turbine generator system on the basis of field tests,"IEEE Trans. Power Delivery, vol. 25, no. 4, pp. 3035–3043, Oct. 2010.

[4] D. S. Gazzana, A. Smorgonskiy, N. Mora, A. Sunjerga, M. Rubinstein, and F. Rachidi, "An experimental field study of the grounding system response of tall wind turbines to impulse surges," Electric Power System Research, vol. 160, pp. 219–225, 2018.

[5] R. Alipio, D. Conceição, R. N. Dias, S. Visacro, and K. Yamamoto, "The effect of frequency dependence of soil electrical parameters on the lightning performance of typical wind-turbine grounding systems," in Proc. XIV International Symposium on Lightning Protection (SIPDA 2017), Natal, Brazil, 2017, pp. 353–358.

[6] R. Alipio, D. Conceição, A. De Conti, K. Yamamoto, R. N. Dias, and S. Visacro, "A comprehensive analysis of the effect of frequency-dependent soil electrical parameters on the lightning response of wind-turbine grounding systems," Electric Power System Research, under review.

[7] R. Alipio, M. A. O. Schroeder, and M. M. Afonso, "Voltage distribution along earth grounding grids subjected to lightning currents," IEEE Trans. Industry Applications, vol. 51, no. 6, pp. 4912–4916, Nov./Dec. 2015.

[8] Md. R. Ahmed and M. Ishii, "Effectiveness of interconnection of wind turbine grounding influenced by interconnection wire," in 2012 International Conference on Lightning Protection (ICLP 2012), Vienna, Austria, 2012, pp. 1–6.

[9] L. Prikler, H.K. Hoidalen, ATPDraw Manual, Version 5.6, 2009.

[10] A. De Conti, S. Visacro, A. Soares, and M. A. O. Schroeder, "Revision, extension and validation of Jordan's formula to calculate the surge impedance of vertical conductors," IEEE Trans. Electromagn. Compat., vol. 48, n. 3, pp. 530–536, Aug. 2006.

[11] C. M. Portela, "Measurement and modeling of soil electromagnetic behavior," in Proc. IEEE Int. Sym. Electromagnetic Compatibility, Seattle, WA, 1999, pp. 1004–1009.

[12] R. Alipio and S. Visacro, "Modeling the frequency dependence of electrical parameters of soil," IEEE Trans. Electromagnetic Compatibility, vol. 56, no. 5, pp. 1163–1171, Oct. 2014.

[13] S. Visacro and A. Soares Jr., "HEM: a model for simulation of lightning-related engineering problems," IEEE Trans. Power Delivery, vol. 20, no. 2, pp. 1026–1208, Apr. 2005.

[14] B. Gustavsen and A. Semlyen, "Rational approximation of frequency domain responses by vector fitting," IEEE Trans. Power Delivery, vol. 14, pp. 1052–1061, July 1999.

[15] A. De Conti, R. Alipio, Single-port equivalent circuit representation of grounding systems based on impedance fitting," accepted for publication on IEEE Trans. Electromagnetic Compatibility, 2018, doi: 10.1109/TEMC.2018.2870730.

[16] B. Gustavsen, "Computer code for rational approximation of frequency dependent admittance matrices," IEEE Trans Power Delivery, vol. 17, no. 4, pp. 1093–1098, Oct.2002.

[17] E. D. Sunde, Earth Conduction Effects in Transmission Systems, 2nd ed. New York: Dover, 1968.

[18] A. De Conti and S. Visacro, "Analytical representation of single- and double-peaked lightning current waveforms," IEEE Trans. Electromagnetic Compatibility, vol. 49, no. 2, pp. 448–451, May 2007.

[19] K. Berger, R. B. Anderson, and H. Kroninger, "Parameters of lightning flashes," Electra, no. 80, pp. 223–237, 1975.

[20] R. Alipio and S. Visacro, "Frequency dependence of soil parameters: effect on the lightning response of grounding electrodes," IEEE Trans. Electromagnetic Compatibility, vol. 55, no. 1, pp. 132–139, Feb. 2013.

[21] R. Alipio, M. T. Correia de Barros, M. A. O. Schroeder, and K. Yamamoto, "A comprehensive analysis of the lightning and low-frequency performance of wind farm grounding systems," Electric Power System Research, under review.